

# Indoor Localization with Channel Impulse Response Based Fingerprint and Nonparametric Regression

Yunye Jin, *Student Member, IEEE*, Wee-Seng Soh, *Member, IEEE*, and Wai-Choong Wong, *Senior Member, IEEE*

**Abstract**—In this paper, we propose a fingerprint-based localization scheme that exploits the location dependency of the channel impulse response (CIR). We approximate the CIR by applying Inverse Fourier Transform to the receiver’s channel estimation. The amplitudes of the approximated CIR (ACIR) vector are further transformed into the logarithmic scale to ensure that elements in the ACIR vector contribute fairly to the location estimation, which is accomplished through Nonparametric Kernel Regression. As shown in our simulations, when both the number of access points and density of training locations are the same, our proposed scheme displays significant advantages in localization accuracy, compared to other fingerprint-based methods found in the literature. Moreover, absolute localization accuracy of the proposed scheme is shown to be resilient to the real time environmental changes caused by human bodies with random positions and orientations.

**Index Terms**—Indoor localization, fingerprinting, channel impulse response, nonparametric kernel regression.

## I. INTRODUCTION

The ability to accurately locate a mobile device in the indoor environment has many applications in retail, healthcare, and entertainment industries. Although the Global Positioning System (GPS) does not work well indoors, the proliferation of various mobile devices and their associated wireless infrastructures have created new opportunities for the realization of effective indoor localization systems.

Fingerprint-based schemes are widely adopted for indoor localization purpose. In a typical fingerprint-based system, a set of “training locations” are chosen in the service area. During an off-line “training phase”, location-dependent signal parameters, most commonly received signal strength (RSS) values, are measured by several access points (APs) for each training location. The measured RSS values for a training location are concatenated into a vector, known as the fingerprint vector, for that particular location. During the online localization phase, various methods can be applied to estimate the target device’s location when the online RSS values of the device are collected. However, in order to reduce hardware cost and interference, it is desirable to construct the localization system based on the existing indoor wireless infrastructure, in which a small number of APs are deployed to provide communication coverage over a large area. Since each AP in

such a system contributes only one dimension to the fingerprint vector, the resulting fingerprint vector may be too low in dimension to distinguish locations over a large area.

In this paper, we propose a novel location fingerprint based on the amplitudes of the approximated channel impulse response (ACIR) vector, which has much higher dimension with the same number of APs compared to the RSS fingerprint. The high dimension and the strong location dependency have given the ACIR higher capacity to distinguish locations. However, as our analysis will show, those elements of the decimal-scale ACIR vector that correspond to larger delays inherently contribute less to the location estimate because of propagation path loss. We therefore transform the ACIR into logarithmic scale to ensure that each element within the fingerprint vector contributes fairly to the location estimation. Nonparametric Kernel Regression (NKR) method with a generalized bandwidth matrix formula is then applied for location estimation.

The rest of the paper is organized as follows. Section II summarizes the related work in localization systems. Section III presents the research methodology in detail, including the proposed fingerprint, the localization algorithm, and the logarithmic transform. Performance of the proposed method under different conditions are simulated and discussed in Section IV. Finally, we conclude our work and point out future directions in Section V.

## II. RELATED WORK

Most of the localization methods proposed in the literature can be classified into two categories, namely, trilateration and fingerprinting.

The resolution of Time-of-Arrival (ToA) based trilateration methods are dominated by the system bandwidth [1], [2]. Although Ultra-Wide-Band (UWB) receivers [3] and wideband receivers with enhanced sampling rates [4] can achieve high ToA resolution, their operating ranges are usually limited to reduce interference. In addition, Non-Line-of-Sight (NLoS) conditions are very common indoors. Methods that utilize NLoS arrival signals directly (i.e. without prior measurements) for localization [5], [6] require accurate knowledge of bidirectional ToA, Angle-of-Arrival (AoA), and Angle-of-Departure (AoD). Algorithms for estimating these parameters in heavy multipath environment, such as MUSIC [7] and ESPRIT [8], require antenna arrays with a large number of array elements on transceivers, which greatly increases the cost of the system. More importantly, in the presence of indoor near-field propagation and coherent multipath signals, efficient methods such as MUSIC and ESPRIT are not directly

The authors are with the Department of Electrical and Computer Engineering, National University of Singapore.

E-mail: {g0700214, weeseng, elewwcl}@nus.edu.sg

This research work is supported by National Research Foundation project grant NRF2007IDM-IDM002-069 on “Life Spaces”.

Manuscript received on February 9, 2009; revised on June 14, August 31, and December 1, 2009.

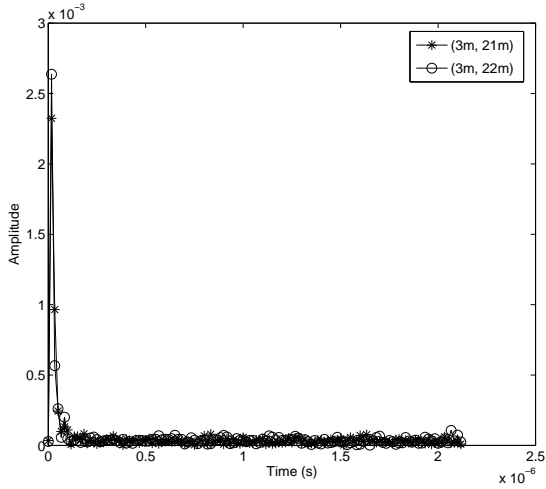


Fig. 1. ACIR vectors with transmitters located 1 m apart, at 60 MHz.

applicable. Instead, we have to resort to algorithms which are much more expensive in terms of computation and hardware [9], [10], [11], [12].

One of the earliest fingerprinting methods, the  $K$  Nearest Neighbor (KNN) scheme [13], returns the location estimate as the average of the coordinates of the  $K$  training locations whose fingerprint vectors have shortest Euclidean distances to the online RSS vector. In [14], the  $K$  nearest neighbors are weighted by the reciprocal of their signal space Euclidean distance to the online RSS vector. Both [15] and [16] have taken the probabilistic approach, in which the training data are used to construct probability density functions (pdf) for the location and the fingerprint vectors. Their mathematical expressions of the location estimates are equivalent to the Nadaraya-Watson Kernel Regression estimator [17]. However, both [15] and [16] assume that the elements of the fingerprint vector are statistically independent from each other for the simplicity of computation, which may not be true in general.

In [18], fine resolution indoor channel impulse response (CIR) has been collected using a channel sounder and a spectrum analyzer, operating at a very high bandwidth (200 MHz). A vector of features concerning the power delay characteristics are extracted from the CIR as the location fingerprint. An Artificial Neural Network (ANN) is trained using the training data to predict location when given an online feature vector. Although it has achieved good localization accuracy, this scheme has its own limitations. First, the cost, physical size and weight, and system bandwidth of the devices are unacceptable in a ubiquitous computing context. Secondly, after the fine resolution measurement is obtained, several features were extracted, which is not an efficient utilization of resources devoted to obtain the fine resolution CIR in the first place. Moreover, some features, such as mean excess delay, root mean square of excess delay, and overall gain of channel, are parameters regarding the entire delay spread. In order to acquire such features, a lower bandwidth may be sufficient. However, [18] has not conducted performance study with varying system bandwidth.

Note that, two-phase localization methods involving training or other prior measurements are also applicable in the outdoor

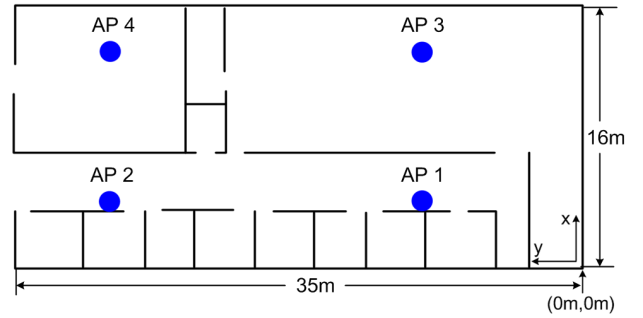


Fig. 2. Simulation testbed.

scenarios, as proposed in [19], [20], and [21]. Although collecting prior measurements for a large outdoor area is more labor and time consuming, such systems have clear advantages in outdoor urban areas where NLoS conditions are common.

### III. PROPOSED METHOD

#### A. Channel Impulse Response Based Fingerprint

Channel impulse response, which completely characterizes the multipath channel and preserves the location dependency [22], is a good choice for location fingerprint. In order to make the localization service more cost-effective and accessible for users of both existing and upcoming wideband OFDM technologies with different system bandwidths, we propose to approximate the CIR from the receiver's channel estimation result. In OFDM systems, channel estimation can be seen as a vector of  $N$  complex elements describing the channel in the frequency domain, where  $N$  is the number of sub-carriers [23]. The time domain CIR is approximated by taking the Inverse Fourier Transform (IFT) of the frequency domain discrete channel estimation vector. Our proposed fingerprint in this paper is based on the *amplitudes* of the approximate CIR vector. Fig. 1 shows the resemblance between two ACIR vectors collected from two transmitters located 1 m apart from each other in our simulation testbed, at a system bandwidth of 60 MHz. (The map of the testbed is shown in Fig. 2 with the coordinate axes, dimensions, and the origin indicated).

As shown also in Fig. 1, the time range of the ACIR vector is inefficiently large. The bandwidth of the system is 60 MHz in this case, yielding a time resolution of 16.67 ns. In this paper, we have used  $N = 128$  for the IFT. Therefore the overall time range is 2133.7 ns. However, the maximum excess delay of indoor channel,  $\tau_{\max}$ , is usually smaller than 500 ns, which corresponds to at most the first 30 time samples in this case. Therefore, the remaining 98 samples are irrelevant for localization purpose. When the Signal-to-Noise-Ratio (SNR) is not high enough, the receiver Additive White Gaussian Noise (AWGN) at these time samples will only make the accuracy worse. As system bandwidth goes higher, the time resolution becomes better and the number of irrelevant time samples becomes smaller. Therefore, based on the system bandwidth, a reasonable number of relevant time samples should be chosen for the sake of computation efficiency and accuracy. In this paper, we preserve the first  $\lfloor \frac{\tau_{\max}}{1/B} \rfloor$  samples in the ACIR vectors for localization purpose, where  $\tau_{\max}$  can be determined

by experimental measurement or simulation for each specific testbed, and  $B$  is the system bandwidth in Hz.

### B. System Implementation Issues

Currently, the receiver channel estimation result is not accessible in off-the-shelf products. However, hardware/firmware modifications can be made in the future to reveal the channel estimation result, which is demanded by more and more localization methods [2], [18]. Alternatively, the raw samples of the received signal at the output of the receiver Analog-to-Digital Converter (ADC) can be used for CIR approximation through special hardware interfaces. The latter approach is adopted in [24] experimentally. However, the authors of [24] have used the debug version of the Intel Pro/Wireless adapter, which is restricted for their internal debugging and research purpose and not commercially available.

### C. Localization by Nonparametric Kernel Regression

Assume that there are  $M$  APs installed in the service area, and  $L$  training locations with 2-D location coordinates,  $\mathbf{c}_l, l = 1, 2, \dots, L$ . During the off-line training phase, the ACIR vectors collected by the  $M$  APs at the training location  $\mathbf{c}_l$  are concatenated and denoted as  $\mathbf{s}_l$ . During the online localization operation, the ACIR vectors collected by the  $M$  APs are concatenated in the same order and denoted as  $\mathbf{s}$ . Let  $D$  denote the dimension of the concatenated ACIR vector. Let the  $D \times D$  matrix,  $\mathbf{C}$ , denote the sample covariance matrix of the fingerprint vectors,  $\mathbf{s}_1, \mathbf{s}_2, \dots, \mathbf{s}_L$ .

The localization task is to find an estimator  $\hat{\mathbf{c}}$ , for the actual location  $\mathbf{c}$ , based on the observed online signal parameter vector  $\mathbf{s}$ . Probabilistic localization methods, such as those in [15] and [16], normally use the conditional expectation,  $\hat{\mathbf{c}} = E\{\mathbf{c}|\mathbf{s}\}$ , as the estimator, which minimizes the conditional mean square error [25]. Notice that,

$$E\{\mathbf{c}|\mathbf{s}\} = \frac{\int \mathbf{c}f(\mathbf{c}, \mathbf{s}) d\mathbf{c}}{\int f(\mathbf{c}, \mathbf{s}) d\mathbf{c}}. \quad (1)$$

The computation of  $E\{\mathbf{c}|\mathbf{s}\}$  requires exact knowledge of the joint pdf,  $f(\mathbf{c}, \mathbf{s})$ , which is usually not available in practice. However, from the training phase, we have obtained  $L$  pairs of training data,  $(\mathbf{c}_l, \mathbf{s}_l), l = 1, 2, \dots, L$ . When the online user signal parameter vector  $\mathbf{s}$  is collected,  $E\{\mathbf{c}|\mathbf{s}\}$  can be approximated by the Nadaraya Watson Kernel estimator [17],

$$E\{\mathbf{c}|\mathbf{s}\} \approx \frac{\sum_{l=1}^L \mathbf{c}_l K_{\mathbf{H}_s}(\mathbf{s} - \mathbf{s}_l)}{\sum_{l=1}^L K_{\mathbf{H}_s}(\mathbf{s} - \mathbf{s}_l)}, \quad (2)$$

where,

$$K_{\mathbf{H}_s}(\mathbf{s} - \mathbf{s}_l) = \frac{1}{\det(\mathbf{H}_s)} K[\mathbf{H}_s^{-1} \cdot (\mathbf{s} - \mathbf{s}_l)]. \quad (3)$$

The function  $K(\mathbf{y} - \mathbf{z})$  is known as the kernel function. Generally, its value is larger when  $\mathbf{y} - \mathbf{z}$  is smaller in all dimensions. In other words, the more similar  $\mathbf{y}$  and  $\mathbf{z}$  are, the larger the resulting kernel function's value. Intuitively, the Nadaraya-Watson kernel estimator is the normalized weighted average of the training locations' coordinates. A training

location with a fingerprint vector more/less similar to the online ACIR vector receives a higher/lower weight.

In this paper, we adopt the popular Gaussian kernel function,

$$K(\mathbf{y} - \mathbf{z}) = \frac{1}{(2\pi)^{D/2}} \exp\left[-\frac{1}{2} (\mathbf{y} - \mathbf{z})^T \cdot (\mathbf{y} - \mathbf{z})\right]. \quad (4)$$

The  $D \times D$  matrix  $\mathbf{H}_s$  is called ‘‘bandwidth matrix’’. It controls the shape and orientation of the kernel function. Note that ‘‘bandwidth’’ here refers to the spread of the kernel. It should not be confused with the system bandwidth in the RF spectrum. The choice of bandwidth matrix is critical to the accuracy of the kernel estimator. For simplicity of computation, both [15] and [16] have chosen a diagonal bandwidth matrix so that only  $D$  kernel bandwidth parameters need to be selected. This is implicitly assuming that the elements in the fingerprint vector are independent from each other. In this paper, we drop this assumption of independence between the fingerprint vector elements and use the multivariate generalization of the Scott's Rule of Thumb for bandwidth selection [26],

$$\mathbf{H}_s = L^{-1/(D+4)} \mathbf{C}^{1/2}, \quad (5)$$

in which  $L$  is the size of training data set,  $D$  is the dimension of the concatenated fingerprint vector, and  $\mathbf{C}$  is the sample covariance matrix. This formula of bandwidth matrix computation takes into consideration the general statistical dependence between the fingerprint vector elements by first transforming them using their sample covariance matrix.

More information on the NKR techniques can be found in [17], [26], and [27].

### D. Regional Smoothing

We apply a simple regional smoothing technique in order to smooth out the individual variations among fingerprint vectors collected within close proximity while preserving their common location dependency. For each training location  $\mathbf{c}_l$ , the smoothed ACIR fingerprint vector is obtained by taking the average of training ACIR vectors in the set,  $\{\mathbf{s}_k | \|\mathbf{c}_k - \mathbf{c}_l\| \leq r_0\}$ , where the constant  $r_0$  determines the range of the smoothing region. We have found experimentally that a good choice for  $r_0$  is to make it equal to the training grid spacing.

### E. Logarithmic Scale Transformation

In order to understand the effect of transforming the decimal scale ACIR vector into logarithmic scale, consider an online ACIR vector,  $\mathbf{h} = [h_1, h_2, \dots, h_N]^T$ , which is the discrete time domain description of the multipath channel's amplitude gain at delay time instants,  $nT_s, n = 1, 2, \dots, N$ , where  $T_s$  is symbol duration. For any  $n$ , the amplitude gain  $h_n$  can be expressed as the product of two terms, which will be described below.

The first term is the amplitude gain purely caused by propagation path loss and antenna characteristics. Assume that a signal  $x(t)$  is transmitted at time instant 0. The multipath version of the transmitted signal received at time instant  $nT_s$  will be,  $a(nT_s) \cdot x(t - nT_s)$ , where  $a(nT_s)$  is the gain purely

caused by propagation path loss. If the transmitted power is  $P_0$ , we have,

$$P_0 = \frac{1}{T} \int_0^T |x(t)|^2 dt, \quad (6)$$

where  $T$  is the time over which the power is measured. The power of the signal received at time instant  $nT_s$  will be,

$$\begin{aligned} P_n &= \frac{1}{T} \int_{nT_s}^{nT_s+T} |a(nT_s) \cdot x(t - nT_s)|^2 dt \\ &= |a(nT_s)|^2 \cdot \frac{1}{T} \int_{nT_s}^{nT_s+T} |x(t - nT_s)|^2 dt \\ &= |a(nT_s)|^2 \cdot P_0 \end{aligned} \quad (7)$$

On the other hand, the overall distance travelled by the signal received at  $nT_s$  seconds after transmission is  $d = v \cdot nT_s$ , where  $v$  is the propagation speed of the RF signal in the medium. Here, we assume that the differences in propagation speeds among different media are negligible. Since we are only considering the pure effects of propagation path loss and antenna characteristics here, by Friis transmission formula [28], we have,

$$P_n = G_a G_b \left( \frac{\lambda}{4\pi d} \right)^2 P_0, \quad (8)$$

where  $G_a$  and  $G_b$  are the gains of transmitter and receiver antennas respectively, and  $\lambda$  is the wavelength. Using (7) and (8), the amplitude gain at delay instant  $nT_s$  purely caused by propagation path loss and antenna characteristics is therefore,

$$|a(nT_s)| = \frac{\sqrt{G_a G_b} \lambda}{4\pi v} \cdot \frac{1}{nT_s}. \quad (9)$$

The second term is the amplitude gain caused by the penetrations, reflections, and diffractions experienced by the signal travelling through the indoor environment. The location dependency is mainly caused by this term. We model the aggregated result of these phenomena by  $\alpha(nT_s)$  for the multipath version of the signal received at  $nT_s$ . Note that if there is no multipath signal received at  $nT_s$ ,  $\alpha(nT_s) = 0$ . Therefore, the overall amplitude gain caused by the indoor channel on a signal that is received at time  $nT_s$  is,

$$h_n = \alpha(nT_s) \cdot \frac{\sqrt{G_a G_b} \lambda}{4\pi v} \cdot \frac{1}{nT_s}, \quad (10)$$

for  $n = 1, 2, \dots, N$  in the online ACIR vector  $\mathbf{h}$ .

The location estimation in (2) involves computing kernel functions using the online ACIR vector and every fingerprint ACIR vector. Consider any fingerprint ACIR vector,  $\mathbf{g} = [g_1, g_2, \dots, g_N]^T$ , whose  $n^{\text{th}}$  element can be expressed as,

$$g_n = \beta(nT_s) \cdot \frac{\sqrt{G_a G_b} \lambda}{4\pi v} \cdot \frac{1}{nT_s}, \quad (11)$$

where  $\beta(nT_s)$  accounts for the aggregated amplitude gain other than propagation path loss, introduced by the indoor channel on the multipath version of the signal received at  $nT_s$ . When computing  $\mathbf{h} - \mathbf{g}$  for the kernel function, the difference at the  $n^{\text{th}}$  vector element is,

$$\begin{aligned} h_n - g_n &= \alpha(nT_s) \cdot \frac{\sqrt{G_a G_b} \lambda}{4\pi v} \cdot \frac{1}{nT_s} \\ &\quad - \beta(nT_s) \cdot \frac{\sqrt{G_a G_b} \lambda}{4\pi v} \cdot \frac{1}{nT_s} \\ &= [\alpha(nT_s) - \beta(nT_s)] \cdot \frac{\sqrt{G_a G_b} \lambda}{4\pi v} \cdot \frac{1}{nT_s}. \end{aligned} \quad (12)$$

For a given SNR and bandwidth condition, as long as the ACIR vector length is still within the relevant range, the  $\alpha(nT_s)$  and  $\beta(nT_s)$  values for all  $n$  should be treated with equal importance for distinguishing locations. However, as seen in (12), simply taking the difference between the corresponding vector elements in the decimal scale ACIRs leaves  $n$  in the denominator. This means that the contribution from the channel amplitude gains with larger delays, corresponding to those elements with larger indices in the ACIR vector, is unnecessarily reduced due to a larger  $n$ . If we transform the elements of the two ACIR vectors to the logarithmic scale, we have,

$$\begin{aligned} \log h_n - \log g_n &= [\log \alpha(nT_s) + \log \left( \frac{\sqrt{G_a G_b} \lambda}{4\pi v} \cdot \frac{1}{nT_s} \right)] \\ &\quad - [\log \beta(nT_s) + \log \left( \frac{\sqrt{G_a G_b} \lambda}{4\pi v} \cdot \frac{1}{nT_s} \right)] \\ &= \log \alpha(nT_s) - \log \beta(nT_s). \end{aligned} \quad (13)$$

As can be seen in (13), the difference between  $\log h_n$  and  $\log g_n$  is not scaled by the time index  $n$  anymore. In other words, all elements in the ACIR vector within the relevant time range contribute evenly to the kernel computation and the location estimation. It should be noted that, the cancellation of the time index factor can also be achieved by directly dividing  $h_n$  by  $g_n$ . The two methods are equivalent in this case. However, in order to be consistent with the kernel function computation, we take the logarithmic transformation approach.

#### IV. SIMULATIONS AND DISCUSSIONS

Since the channel estimation results are currently not accessible in off-the-shelf wireless adapters, the localization performance of the proposed method is evaluated through simulations in our paper as a first step. We have chosen a 3-D ray-tracing based simulator, the Radiowave Propagation Simulator (RPS) [29], in order to closely emulate the indoor propagations. RPS is able to generate fine-resolution CIR, taking into consideration the effects of the penetrations, reflections, and diffractions experienced by an RF signal, after the environment model, transmitter-receiver locations, antenna characteristics, and carrier frequency are specified by the user. The accuracy of RPS simulator has been verified via comparison with real indoor experimental measurements in [30]. Transceiver operations such as sampling and channel estimation are simulated using MATLAB.

We have constructed the 3-D model for one part of our campus. It is 16 m  $\times$  35 m in dimension, including two laboratory rooms on one side, eight staff offices on the other, and a corridor between them. This indoor simulation testbed is a mixture of both LoS and NLoS propagation conditions. The material characteristics of the testbed elements affecting the RF propagation are summarized in Table I, in which  $\epsilon_{Re}$  and  $\epsilon_{Im}$  are the real and imaginary parts of the relative permittivity of the material respectively. As shown in Fig. 2, the two shaded circles at the bottom correspond to the locations of the actual Wi-Fi APs deployed in the building for wireless communication coverage, while the two on the top are added to the testbed to study the effects of varying the number of APs on the localization accuracy. The APs and the user mobile device are placed 2 m and 1.2 m above the ground, respectively. We

TABLE I  
MATERIAL CHARACTERISTICS FOR TESTBED

Object	$\epsilon_{Re}$	$\epsilon_{Im}$	Thickness (m)
Floor and Ceiling	4	-0.2	0.5
Wall	4	-0.4	0.15
Human Body	11	-2.04	0.25

assume that all the transmitters and receivers are equipped with omni-directional antennas. The carrier frequency is set to 5 GHz and the transmission power is set to 20 dBm.

Training grid spacing of 1 m [18] or 2 m [15], [16] are commonly chosen for indoor fingerprint-based systems. In this paper, we use 1.5 m training grid spacing to evaluate the localization accuracy of the proposed system under varying factors such as system bandwidth, number of APs, and number of people in the testbed which create random environmental changes. We also study the effect of changing the training density by setting the training grid spacing from 1 m to 2.5 m, with a 0.5 m step size. There are 173 testing locations picked in the testbed. Twenty testing samples are taken at each testing location, resulting in 3460 testing samples overall in each set of simulations. Note that, in order to compare the performance of the schemes under the variations of different factors, the average localization error of these 3460 testing samples are used as the metric. Whenever applicable, the 95% confidence interval [31] for each data point is also shown in the figures.

#### A. Performance with Varying System Bandwidth

The localization accuracy of the proposed logarithmic-scale ACIR fingerprint with Nonparametric Kernel Regression (LOG-ACIR-NKR) is first compared with three other methods, namely, RSS fingerprint with Kernel distance method (RSS-Kernel), as described in [16], decimal-scale ACIR fingerprint with Nonparametric Kernel Regression (ACIR-NKR), and decimal-scale ACIR fingerprint with General Regression Neural Networks (ACIR-GRNN), generalized from [18], with system bandwidth increasing from 20 MHz to 200 MHz, at a step size of 20 MHz, when two APs, 1.5 m training grid spacing are used. In order to implement the ACIR-GRNN scheme, five features are extracted from the ACIR vector, namely, the mean excess delay, the root mean square (rms) of the excess delay, the overall power gain of the channel, as well as the power gain and delay of the first arrival path. A GRNN [32] is used to map features to location coordinates.

As shown in Fig. 3, the proposed LOG-ACIR-NKR scheme has achieved much higher localization accuracy compared to the RSS-Kernel scheme and the ACIR-GRNN scheme for all the system bandwidths tested. It is important to note that, the logarithmic transformation is critical to the superior advantage, as can be shown by the huge difference in performance between LOG-ACIR-NKR scheme and the ACIR-NKR scheme. As explained earlier, this is because the elements in the logarithmic scale ACIR vector now have fair contributions to the location estimation.

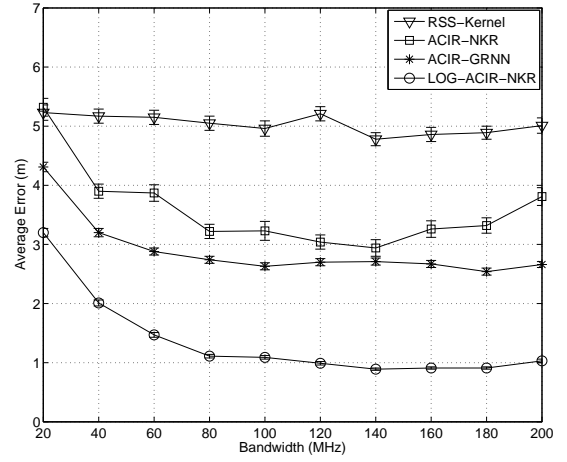


Fig. 3. Localization accuracy vs. system bandwidth (using only AP 1 and AP 2).

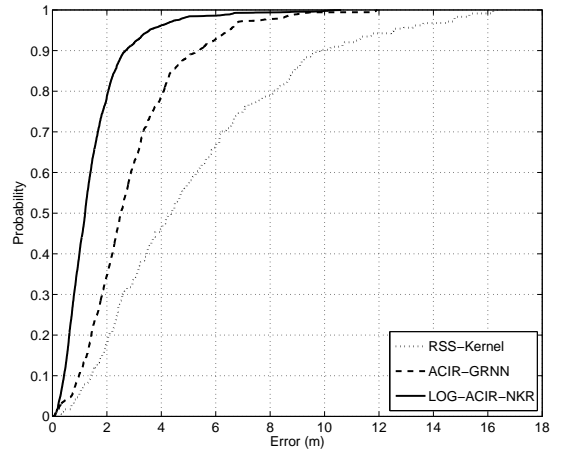


Fig. 4. Cumulative error probability (using only AP 1 and AP 2).

#### B. Cumulative Error Distribution

Fig. 4 shows the cumulative error distribution functions of RSS-Kernel, ACIR-GRNN, and the proposed LOG-ACIR-NKR, when two APs, a training grid spacing of 1.5 m, and a system bandwidth of 60 MHz are used. As can be seen, the proposed scheme achieves a localization error under 2.05 m for 80% of the testing samples, which is significantly smaller than those of ACIR-GRNN (4.09 m) and RSS-Kernel (8.15 m).

#### C. Effect of Varying Training Location Density

The effect of varying training location density can be examined by choosing different subsets of the training locations with different training grid spacing. The localization error of RSS-Kernel, ACIR-GRNN, and LOG-ACIR-NKR at 60 MHz with two APs are shown in Fig. 5. When training grid spacing increases from 1 m to 2.5 m, with a step size of 0.5 m, the performance of all the three methods becomes worse. However, it should be noted that, the error of the proposed LOG-ACIR-NKR scheme with 2.5 m training grid spacing, which corresponds to 78 training locations, is smaller than that of ACIR-GRNN scheme with 1 m training grid spacing, which corresponds to 544 training locations. This means that

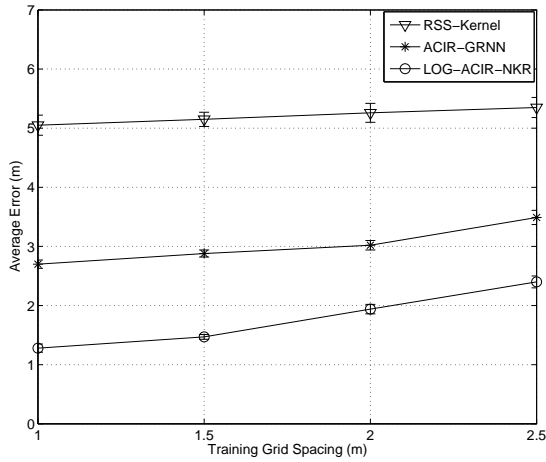


Fig. 5. Localization accuracy vs. training density (using only AP 1 and AP 2).

the proposed LOG-ACIR-NKR scheme is much more efficient in utilizing the available training data.

#### D. Effect of Varying the Number of Access Points

Next, we keep the training grid spacing at 1.5 m, system bandwidth at 60 MHz, and vary the number of APs. As shown in Fig. 6, all the three algorithms benefit from an increase in the number of APs. When there are four APs, the average localization error for RSS-Kernel is 3.23 m, which is comparable with the experimental results presented in the literature for RSS fingerprint-based localization. It should be emphasized that, even with only two APs, the localization error of the proposed LOG-ACIR-NKR scheme is still better than that of the ACIR-GRNN scheme with 4 APs. This result implies that, when we have to construct a localization system in an area where there are limited number of APs, the proposed scheme is a preferred choice.

#### E. Effect of Real Time Variation in Environment

One major cause of real time changes in the environment is the random positions and orientations of human bodies. This is because the human body contains a large amount of water, which is an excellent absorber of RF radiation. In this section, we model the human body by a  $0.5 \text{ m} \times 0.25 \text{ m} \times 1.8 \text{ m}$  cuboid with the same relative permittivity as pure water. As shown in Fig. 7, based on the training data collected when no one is in the testbed, the localization accuracy of RSS-Kernel, ACIR-GRNN, and LOG-ACIR-NKR schemes are tested in cases where different number of people are randomly positioned in the testbed, which operates with 60 MHz bandwidth, two APs, and 1.5 m training grid spacing. For each data point, the average location errors are computed and plotted for 10 random snapshots. In each snapshot, the same number of people are randomly placed and oriented in the testbed. As can be seen in Fig. 7, the performance of all three methods become worse when there are more people in the environment. However, the LOG-ACIR-NKR scheme maintains its superior advantage in absolute localization accuracy among the three

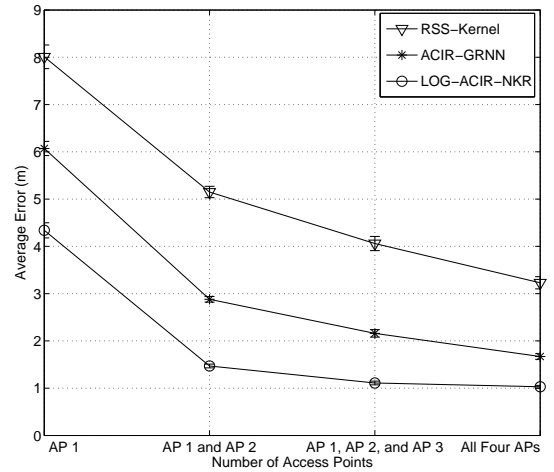


Fig. 6. Localization accuracy vs. number of access points.

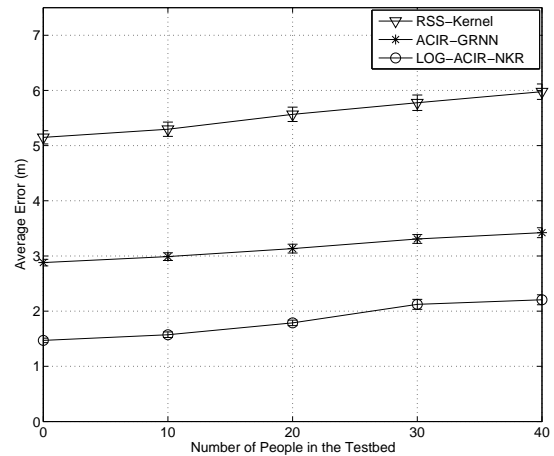


Fig. 7. Localization accuracy vs. number of people randomly placed and oriented in the testbed (using only AP 1 and AP 2).

methods. Even in the random presence of 40 people, it is still able to outperform the ACIR-GRNN scheme with no one in the testbed. Note that, for each data point, the worst-case 95% confidence interval among the 10 snapshots is shown.

#### F. Computation Time

The smoothing and logarithmic transformation of the fingerprint vectors can be pre-computed off-line. During the online location estimation, as can be seen from (2), most of the time is spent on computing the kernel function values for the  $L$  training sample vectors. For each Gaussian kernel computation, the most time-consuming operation is the matrix multiplication in the exponent. Therefore, if the fingerprint vector's dimension is  $D$ , the localization scheme has a complexity  $O(D^2)$ . For our simulation, we have carried out the localization computation in MATLAB, running on a desktop PC with Intel Core 2, 2.83 GHz Quad CPU, and 3 GB RAM. The average time (over 3460 samples) spent in locating one testing sample is 3.33 ms for the proposed fingerprint, when two APs, a training grid spacing of 1.5 m, and a system bandwidth of 60 MHz are used. The absolute overhead incurred in locating a single user

can be very small if a powerful, dedicated localization server is used to implement the proposed scheme.

## V. CONCLUSION AND FUTURE WORK

In this paper, we have proposed a new localization fingerprint based on the ACIR. Compared to other channel-related fingerprints, which require dedicated devices and high bandwidth, this new fingerprint is more cost-effective because it can be efficiently derived from channel estimation results that exist in most modern wireless communication devices. We transform the fingerprint into the logarithmic scale to ensure that the elements of the fingerprint vector contribute fairly to the location estimation. By simulations, we have shown that the combination of logarithmic-scale ACIR fingerprint with NKR displays superior performance advantage when compared to traditional RSS fingerprint based methods, and also the scheme which combines neural network and extracted features from ACIR. The significance of improvement in accuracy is verified under different bandwidth conditions. Simulation results have also shown that, our proposed scheme is not only robust to real time channel variations caused by random positions and orientations of human bodies, but is also more efficient in utilizing hardware infrastructure and training effort, compared to other schemes proposed in the literature.

We suggest several future directions based on this work. First of all, since channel estimation results are currently not accessible in off-the-shelf products, we aim to search or implement transceiver modules with suitable size and RF specifications, in order to verify our proposed method in a realistic and extended testbed. Secondly, the computations of kernel function with all fingerprint vectors in the training database introduce major overhead in the localization process, especially when more than one user needs to be located simultaneously. We therefore need an intelligent database searching technique to reduce the time spent on searching. Moreover, our work in this paper focuses on the task of locating static users. In practice, the users are moving from time to time. Making use of the real time variation of the channel based information for mobile user tracking will be a challenging task.

## ACKNOWLEDGMENT

The authors would like to thank the anonymous reviewers for their valuable comments and suggestions.

## REFERENCES

- [1] K. Pahlavan, X. Li, J. P. Makela, "Indoor geolocation science and technology," *IEEE Communications Magazine*, vol. 40, pp. 112-118, Feb. 2002.
- [2] X. Li, K. Pahlavan, "Super-resolution TOA estimation with diversity for indoor geolocation," *IEEE Trans. Wireless Communication*, vol. 3, pp. 224-234, Jan. 2004.
- [3] J. Y. Lee, R. A. Scholtz, "Ranging in a dense multipath environment using an UWB radio link," *IEEE JSAC*, vol. 20 pp. 1677-1683, Dec. 2002.
- [4] R. Yamasaki, A. Ogino, T. Tamaki, T. Uta, N. Matsuzawa, T. Kato, "TDOA location system for IEEE 802.11b WLAN," in *Proc. IEEE WCNC*, vol. 4, pp. 2338-2343, Mar. 2005.
- [5] H. Miao, K. Yu, M. J. Juntti, "Positioning for NLOS propagation: algorithm derivations and Cramer-Rao Bounds," *IEEE Trans. Vehicular Technology*, vol. 56, no. 5, pp. 2568-2580, Sep. 2007.
- [6] C. K. Seow, S. Y. Tan, "Non-Line-of-Sight localization in multipath environments," *IEEE Trans. Mobile Computing*, vol. 7, no. 5, pp. 647-660, May 2008.
- [7] R. O. Schmidt, "Multiple emitter location and signal parameter estimation," *IEEE Trans. Antennas Propagation*, vol. AP-34, pp. 276-280, Mar. 1986.
- [8] R. Roy, T. Kailath, "ESPRIT - Estimation of signal parameters via rotational invariance techniques," *IEEE Trans. ASSP*, vol. 37, pp. 984-995, Jul. 1989.
- [9] H. Krim, M. Viberg, "Two decades of array signal processing research: the parametric approach," *IEEE Signal Processing Magazine*, vol. 13, iss. 4, pp. 67-94, Jul. 1996.
- [10] E. Cekli, H. A. Cirpan, "Deterministic maximum likelihood method for the localization of near-field sources: algorithm and performance analysis," in *Proc. IEEE ICECS*, vol. 2, pp. 1077-1080, 2001.
- [11] T. J. Shan, M. Wax, T. Kailath, "On spatial smoothing for direction of arrival estimation of coherent signals," *IEEE Trans. ASSP*, vol. 33, iss. 4, pp. 806-811, Apr. 1985.
- [12] H. Wang, M. Kaveh, "Coherent signal-subspace processing for the detection and estimation of angles of arrival of multiple wide-band sources," *IEEE Trans. ASSP*, vol. 33, no. 4, pp. 823-831, Aug. 1985.
- [13] P. Bahl, V. Padmanabhan, "RADAR: An in-building RF-based user location and tracking system," in *Proc. IEEE INFOCOM*, vol. 2, pp. 775-784, Mar. 2000.
- [14] M. Brunato, R. Battiti, "Statistical learning theory for location fingerprinting in wireless LANs," *Computer Networks*, vol. 47, iss. 6, pp. 825-845, Apr. 2005.
- [15] P. Myllymäki, T. Roos, H. Tirri, P. Misikangas, J. Sievänen, "A probabilistic approach to WLAN user location estimation," *International Journal of Wireless Information Networks*, vol. 9, pp. 155-164, Jul. 2002.
- [16] A. Kushki, K. N. Plataniotis, A. N. Venetsanopoulos, "Kernel-based positioning in wireless local area networks," *IEEE Trans. Mobile Computing*, vol. 6, no. 6, pp. 689-705, Jun. 2007.
- [17] D. W. Scott, *Multivariate Density Estimation, Theory, Practice, and Visualization*, Wiley-Interscience, 1992.
- [18] C. Nerguizian, C. Despins, S. Affés, "Geolocation in mines with an impulse response fingerprinting technique and neural networks," *IEEE Trans. Wireless Communications*, vol. 5, pp. 603-611, Mar. 2006.
- [19] C. J. Debono, J. K. Buhagiar, "Neural location detection in wireless networks," in *Proc. European Conference on Wireless Technology*, pp. 133-136, 2004.
- [20] H. Laitinen, T. Nordström, J. Lähteenmäki, "Location of GSM terminals using a database of signal strength measurements," *URSI XXV National Convention on Radio Science*, pp. 88-89, Sep. 2000.
- [21] S. Mazuelas, F. A. Lago, J. Blas, A. Bahillo, P. Fernandez, R. M. Lorenzo, E. J. Abril, "Prior NLOS measurement correlation for positioning in cellular wireless networks," *IEEE Trans. Vehicular Technology*, vol. 58, no. 5, pp. 2585-2591, Jun. 2009.
- [22] T. S. Rappaport, *Wireless Communications, Principles and Practice*, Prentice Hall, 2002.
- [23] J.-J. van de Beek, O. Edfors, M. Sandell, S. K. Wilson, P. O. Börjesson, "On channel estimation in OFDM systems," in *Proc. IEEE VTC*, pp. 815-819, Jul. 1995.
- [24] S. A. Golden, S. S. Bateman, "Sensor measurements for Wi-Fi location with emphasis on time-of-arrival ranging," *IEEE Trans. Mobile Computing*, vol. 6, no. 10, pp. 1185-1198, Oct. 2007.
- [25] I. Rhodes, "A tutorial introduction to estimation and filtering," *IEEE Trans. Automatic Control*, vol. 16, iss. 6, pp. 688-706, Dec. 1971.
- [26] W. Härdle, M. Müller, Stefan Sperlich, A. Werwatz, *Nonparametric and Semiparametric Models*, Springer Series in Statistics, 2004.
- [27] B. W. Silverman, *Density Estimation for Statistics and Data Analysis*, Chapman and Hall, 1986.
- [28] S. R. Saunders, *Antennas and Propagation for Wireless Communication Systems*. John Wiley & Sons, 1999.
- [29] Radioplan Product Overview . [Online]. Available: <http://www.actix.com/Docs/OurProducts/Radioplan/ActixRadioplanProductOverview.pdf>. [Accessed:19 Jan. 2010]
- [30] H. Yang, M. H. A. J. Herben, P. F. M. Smulders, "Indoor radio channel fading analysis via deterministic simulations at 60 GHz," in *Proc. ISWCS*, pp. 144-148, Sep. 2006.
- [31] A. Papoulis, S. U. Pillai, *Probability, Random Variables and Stochastic Processes*, McGraw-Hill, 2002.
- [32] D. F. Specht, "A general regression neural network," *IEEE Trans. Neural Networks*, vol. 2, pp. 568-576, Nov. 1991.



**Yunye Jin** (S'09) received the B.Eng degree (Hons) in computer engineering from National University of Singapore (NUS) in 2007. He is currently working towards the Ph.D degree in the Department of Electrical and Computer Engineering, NUS, with research emphasis on the algorithms and theoretical performance analysis for indoor tracking and localization systems.



**Wee-Seng Soh** (S'95–M'04) received the B.Eng. (Hons) and M.Eng. degrees in electrical engineering from the National University of Singapore in 1996 and 1998, respectively. In 1998, he was awarded the Overseas Graduate Scholarship by the National University of Singapore to study at Carnegie Mellon University, Pittsburgh, PA, where he received the Ph.D. degree in electrical and computer engineering in 2003.

Since 2004, he has been with the Department of Electrical and Computer Engineering, National University of Singapore (NUS), where he is currently an Assistant Professor. Prior to joining NUS, he was a Postdoctoral Research Fellow in the Electrical Engineering and Computer Science Department, University of Michigan. His current research interests are in wireless networks, underwater networks and indoor localization.



**Wai-Choong (Lawrence) Wong** is Professor in the Electrical and Computer Engineering (ECE) Department, National University of Singapore (NUS). He is presently Deputy Director (Strategic Development) of the Interactive and Digital Media Institute at NUS. He was previously Executive Director of the Institute for Infocomm Research (I2R) from Nov. 2002 to Nov. 2006. Since joining NUS in 1983, he served in various positions at the department, faculty and university levels, including Head of the ECE Department from Jan. 2008 to Oct. 2009, Director

of the Computer Centre at NUS from Jul. 2000 to Nov. 2002, Director of the Centre for Instructional Technology, NUS, from Jan. 1998 to Jun. 2000. Prior to joining NUS in 1983, he was a Member of Technical Staff at AT&T Bell Laboratories, Crawford Hill Lab, NJ, USA from 1980 to 1983.

He received the B.Sc. (1st class Honours) and Ph.D. degrees in Electronic and Electrical Engineering from Loughborough University, UK, in 1976 and 1980, respectively. His research interests include wireless networks and systems, multimedia networks, ambient intelligent systems and platforms, and source matched transmission techniques with over 200 publications and 4 patents in these areas. He is co-author of the book on "Source-Matched Mobile Communications". He received the IEEE Marconi Premium Award in 1989, NUS Teaching Award (1989), IEEE Millennium Award in 2000, the e-nnovator Awards 2000, Open Category, and Best Paper Award at the IEEE International Conference on Multimedia and Expo (ICME) 2006.